Intrinsic Connectivity of Hippocampal Subregions of the epileptic patients using T1-w and T2-w MRI

Tongpeng Chu[a], Chunlan Yang[b,*], Min Lu[c], Wenxiao Wu[d], and Shuicai Wu[e]

College of Life Science and Bioengineering, Beijing University of Technology, Beijing, China

[a]chutongpeng@163.com, [b]clyang@bjut.edu.cn, [c]lumin@emails.bjut.edu.cn,

[d]wenxiaowu93@163.com, [e]wushuicai@bjut.edu.cn

*Corresponding author

Keywords: Epilepsy, Hippocampal subregional structural networks, Small-world attributes, Graph theory

Abstract: Hippocampus is heterogeneous and can be divided into subregions with different functions, but the connectivity specificities of the hippocampal subregional structural networks are poorly known. Hence, in this study, we investigated the connectivity of hippocampal subregions at the network level. Then, we analyzed the changes of network attribute between normal group and epileptic group. The results indicate that compared with the normal group, the nodes of the epileptic group were reorganized, and the hippocampal subregional network tended to be modularized. In addition, the correlation matrix and p-value matrix after correction by FDR between the two groups also showed significant differences. The connection matrix of epileptic group shows a tendency of modularization. This is consistent with the results of BC. These findings provide more comprehensive insights for future research into the epilepsy.

1. Introduction

This Epilepsy has been associated with a spectrum of changes in hippocampal shape [1]. Structural abnormalities in the hippocampus are a common finding in epileptic studies [2], and human autopsy studies [3,4] have shown that subregions of the hippocampus are differently affected by neuropsychiatric disorders. Morphometric MRI (magnetic resonance imaging) has been the most efficient tool for studying the progression of structural damage in the human brain. Structural hippocampal connectivity has been widely described, but the connectivity specificities of the hippocampal subregional structural networks are poorly understood.

It is well known that the hippocampus is heterogeneous and can be divided into subregions with different functions, connections to other regions of the brain, and susceptibility to disease [5,6]. The hippocampal parcellation with additional head, body, tail: it mimics the FreeSurfer 6.0 hippocampal module, i.e., no head/body subdivision for the hippocampal subregions [7]. Several histological studies have investigated the afferent and efferent projections of the hippocampus to other parts of the brain [6]. For example, the subicular and hilar/dentate regions, instead of the classically affected CA1 region. are the main shape changes in patients with low-atrophy temporal lobe epilepsy. Hippocampal subregional structural networks could be generated from across-subject covariance of MRI derived morphometric features such as cortical thickness or gray matter volume [8].

We study the hippocampal network topology in healthy subjects and epileptic patients at the subregional level, which may serve as a basis for a better understanding of their physiological functions in health and disease.

2. Materials and Methods

2.1 Participants

Twenty consecutively selected patients with epilepsy confirmed with video–electroencephalography (EEG) and 20 age, gender, and handedness matched healthy controls were studied. All participants had history of focal seizures consistent with epilepsy. Controls had no psychiatric or neurologic disorder that could affect cognitive functioning. The study was approved by the Ethics Committee at Beijing Tiantan Hospital, Capital Medical University. No significant difference in gender and age was found between the two groups. The WAIS-RC (Wechsler adult intelligence scale of China revises) scores were significantly different, including VIQ (verbal intelligence quotient), PIQ (performance intelligence quotient) and FIQ (Full scale intelligence quotient). The demographic characteristics of the controls, the patients with epilepsy are summarized in Table 1.

Table 1 Baseline characteristics

Characteristic	Controls		epilepsy		*p*
	Mean	SD	Mean	SD	
Subjects	20		20		
Sex(M/F)	11/9		8/12		0.379
Handedness(L/R)	2/18		2/18		0.067
Age(years)	29.05	7.86	24	1.84	1.000
WAIS-RC(VIQ-score)	91.45	12.06	113.7	8.66	<0.001*
WAIS-RC(PIQ-score)	96.1	12.28	109.6	10.65	<0.001*
WAIS-RC(FIQ-score)	92.95	11.01	112.9	7.48	<0.001*
Note: * is statistically significant (p <0.05); WAIS-RC: Wechsler adult intelligence scale of China revises; VIQ: verbal intelligence quotient; PIQ: performance intelligence quotient; FIQ: Full scale intelligence quotient.					

2.2 MRI Data Acquisition

Each subject underwent two MR scans (T1-weighted and T2-weighted) at the Neurosurgical Institute of Beijing Tiantan Hospital, Capital Medical University using a Siemens Medical Solutions 3T scanner. First, T1-weighted structural images were acquired (repeat time (TR) = 2300 ms; echo time (TE) = 2.32 ms; inversion time (TI) = 900 ms; flip angle = 8 degrees; field of view (FOV) = 100×100 mm2; 192 slices; slice thickness = 0.9 mm; no gap; matrix = 256×256). Second, T2-weighted structural images were acquired (t2.tirm.cor.dark-fluid.3mm; TR = 9000 ms; TE =81 ms; TI = 2500ms; 25 slices; slice thickness = 3 mm; flip angle = 150 degrees; Spacing Between Slices=3.9; Field of View = 100×100 mm2; matrix = 320×224).

2.3 Segmentation of hippocampal subfields

All the images were preprocessed with FreeSurfer 6.0, which can be downloaded for public online (http://www.freesurfer.net/fswiki/DownloadAndInstall). This software generates an automated segmentation of the hippocampal subfields based on a statistical atlas built primarily upon ultra-high resolution (~0.1 mm isotropic) ex vivo MRI data [9]. This software has three modes of operation, depending on whether you only have a T1 scan or you have an additional MRI volume (any MRI contrast supported) containing the hippocampus. In this study, Mode B: segmentation with an additional scan (T2 scan containing the hippocampus) was used to obtain a more reliable segmentation.

Figure 1 showed a sample multimodal segmentation, computed from a 1mm (isotropic) T1 and a 0.68 x 0.68 x 3.0 mm (coronal) T2 scan, with the different hierarchical levels. The hippocampus is divided into 12 subregions, including parasubiculum, presubiculum, subiculum, CA1, CA3, CA4, GC-ML-DG, molecular_layer, HATA, fimbria, hippocampal_fissure and hippocampal _tail. When

this module has been run, we collected the volumes of the subregions of the hippocampus of all subjects and writed them in a single file - which can be easily analyzed with network subsequently.

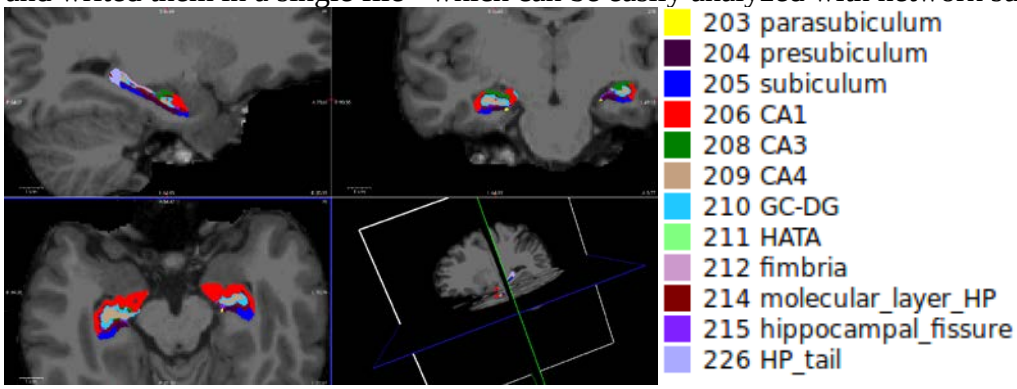

Fig. 1. Segmentation of hippocampal subfields. From left to right, top to bottom show sagittal, coronal, axial and three-dimensional views. The hippocampus is divided into 12 subregions, listed on the right side of the figure and differentiated through different colors. Note: CA2 is always included in CA3.

2.4 Structural Network Generation

We carried out an extra processing step on the volumetric features to eliminate the dimension effect. Consistent with the procedures in [10], we calculated the z-score of the volumetric features and used these values in pearson correlation. We use Pearson's normalized correlation between the hippocampal subregions to generate a R matrix (Pearson correlation coefficient matrix) and a P matrix (p values matrix), because in previous studies, the correlation between Pearson's regional gray volume was found to be a useful measure of structural connectivity [11-13]. The significance of the correlation coefficient in P was corrected by FDR (False discovery rate) [14,15]. In the corrected P matrix, the element with $p<0.05$ was considered to be significantly correlated between the two hippocampal subregions. In contrast, when $p>0.05$, it was considered that there was no correlation between the two hippocampal subregions. Where, the R matrix does not consider the positive and negative of the correlation value, but only considers the strength of the edge, so the resulting matrix is a symmetric matrix. Matrix is retained with full weight because studies have shown that connection strength contains important information about network architecture [16].

Density is the fraction of present connections to possible connections [17]. However, it is not possible to find an optimal density value to construct the correlation matrix. Therefore, brain scientists believe that the most effective and feasible method should set a density range to observe the changes in brain networks within a density range [18,19]. In this study, according to the actual network density range of the two groups, the measurement of network attribute parameters was calculated in the range of 6%-23% network density to ensure the robustness and comparability.

In the hippocampal subregional structural networks, the matrix represents the graph of the subregions as the node, and the correlation strength between the subregions is taken as the edge weight. Figure 2 shows the process of constructing the structural network in the hippocampal subregions.

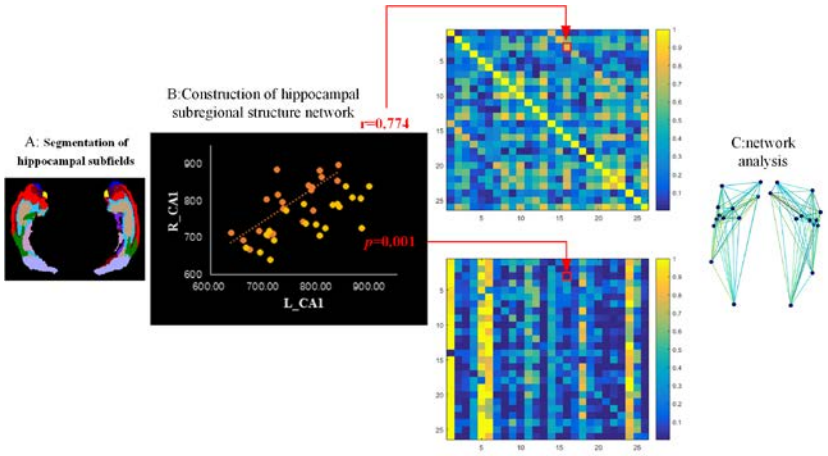

Figure 2. Workflow of this study. A: Segmentation of hippocampal subfields; B: Elements of the R matrix were equivalent to Pearson correlations between normalized hippocampal subregions gray matter volume pairs across subjects and elements of the P matrix were *p* value corrected by FDR (each data point in the display shows one subject); C: Networks were analyzed using various graph theoretic measures.

2.5 Network analysis

The network properties were computed using the Brain Connectivity Toolbox (BCT) [20]. To investigate the difference in hippocampal subregional structural network between patients with epilepsy and normal controls, we conducted a two-sample t-test on the properties of the network. The calculation was performed with IBM SPSS Statistics (version 24.0). The spatial distribution of hubs was visualized using the BrainNet Viewer toolkit [21] (Figure 2C). The multiple comparison was corrected with the false discovery rate (FDR) proposed by [14].

3. Results

3.1 Small World Properties

The hippocampal subregional structural network constructed by the above steps, the network density ranges of the normal group (5%-23%, interval 0.01) and the epilepsy group (6%-38%, interval 0.01) was obtained [22]. Density is the fraction of present connections to possible connections [17].

In this study, the Cp (cluster coefficient), the Lp (shortest path length), and sigma [23] is in the network to calculate the density of 6% to 23% range, to ensure that all the parameters calculation is not based on the density of a certain density value, on the larger degree in addition to select a particular network density error rate (Figure 3a, b, c). The network density shared by both groups was selected to ensure comparability. As shown in figure 3a, b and c, the sigma values of the normal group and the epileptic group were all greater than 1, indicating that they all had small-world properties. The Cp value of the epileptic group was only lower than that of the normal group when the network density was 6%, and higher than that of the normal group when the network density was 7% to 23%; Lp values were larger in the normal group than in the network density of 6% to 14%, and were smaller in the range of 15% to 23%.

3.2 Network Properties

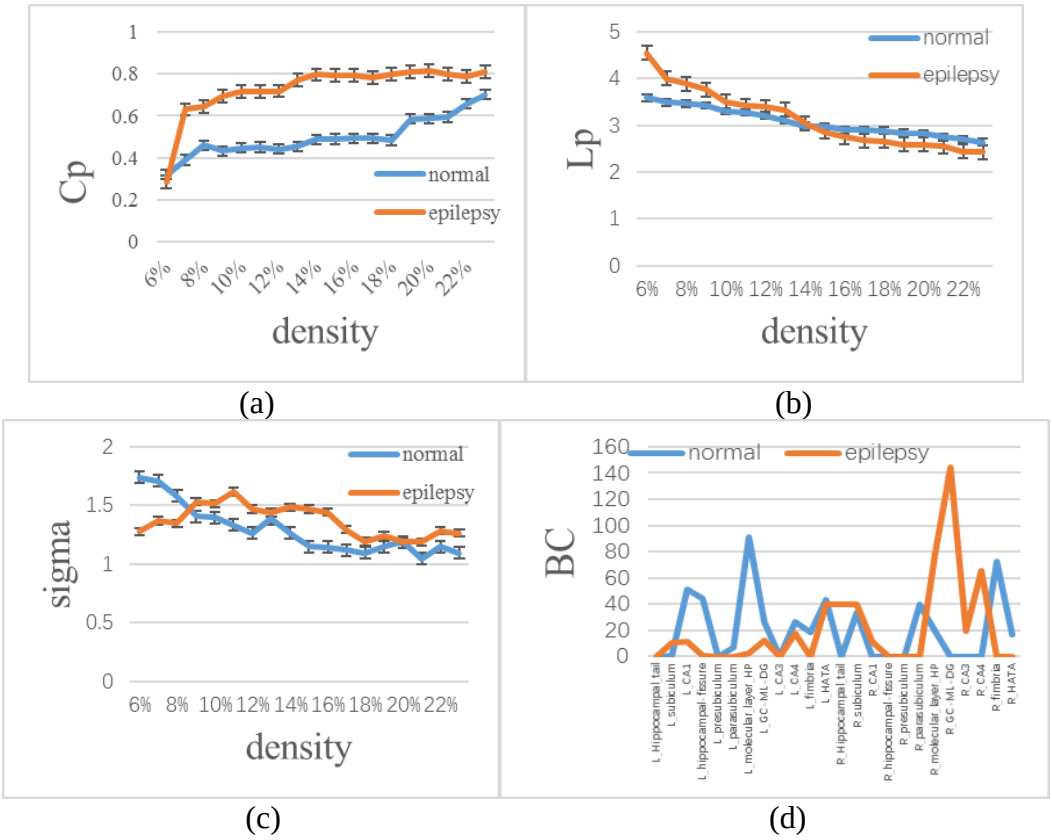

(a) (b)

(c) (d)

Figure 3. Cp value (a), Lp value (b), sigma value (c) and BC value (d), abscissa denotes network density when network density is between 6% and 23% in the epilepsy group and normal group.

BC is the most widely used metric to measure the importance of a node in a network [24]. The BC of each node (Figure 3d), that pass through it, was calculated in order to characterize the centrality of the different hippocampal subregions [25]. In addition, the calculation of degree of BC (Betweenness Centrality) is based on the network density (16%), ensures that each group have the same number of edges and nodes, to ensure that the final calculated results reflect the network topology between two groups in the face of the change of the external attack, not just confined to the lower levels of nodes and edges of correlation contrast [18,19]. Then nodes are arranged from low to high according to the center of the node. Five nodes with the highest BC are chosen [25]. They are called hubs. In the normal group, hubs are: L_CA1, L_molecular_layer_HP, L_HATA, R_parasubiculum and R_fimbria. In the epilepsy group, hubs are: L_CA4, R_molecular_layer_HP, R_GC-ML-DG, R_CA3 and R_CA4. In this case, the L is for the left, and the R is for the right.

As shown in figure 3c, compared with the normal group, the nodes of the epileptic group were reorganized, and the hippocampal subregional network tended to be modularized. In addition, the correlation matrix and p-value matrix after correction by FDR between the two groups also showed significant differences (Figure 4). The connection matrix of epileptic group shows a tendency of modularization. This is consistent with the results of BC.

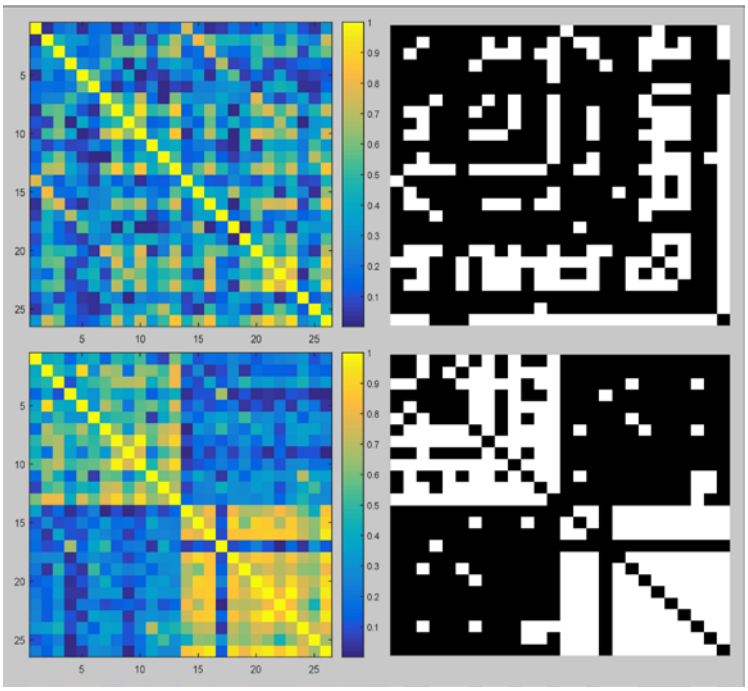

Figure 4. The R matrix (left side figure) and binary P matrix after correction by FDR (right side figure) for the normal control group and the epilepsy group. The color bar shows the strength of the correlation with yellow as strong correlation. Black elements in binary P matrix indicate effective connections within 95% confidence interval.

4. Discussion

The sigma values of the normal group and the epileptic group were all greater than 1, indicating that they all had small-world properties. The small-world attribute is represented by higher Cp and shorter Lp [20], which not only has the high efficiency of processing local information in regular network, but also has the high efficiency of information transmission and integration in random network [26]. Cp and Lp are believed to be related to the cognitive ability of the brain, such as spatial resolution, executive ability, and brain functions such as intelligence [27]. The analysis of the above network properties also indicated that the topological parameters of the epileptic group were changed. This paper confirms these views from the network level.

Compared with the normal group, the sigma values in the epileptic group were higher in the density of the network between 9% and 23%, indicating that the properties of the network in the small world were reduced and the efficiency of global information integration and transmission was reduced. Figure 4 shows that the network tends to be modularized, with the connection between the left and right hippocampal subregions reduced and the internal connection within the hippocampal subregions enhanced, which may be related to the compensation mechanism of the human body [28]. However, this disruption and change in the network structure may be the cause of the decline in the IQ of patients with epilepsy.

5. Conclusions

The main purpose of this paper is to analyze the differences of hippocampal subregional structural networks between normal group and epileptic group by graph theory. The results showed that there was a wide range of abnormalities in the hippocampal subregional structural networks in the epileptic group. The network topology and core nodes have been changed. The decreased network connection of the left and right hippocampal regions and the increased network connection of the internal hippocampal subregions may be related to the compensation mechanism of the brain. This change in network structure is likely to be a major factor in the decline in IQ (both VIQ and PIQ) in epileptic

patients. This paper can be used as a reference for future studies on the function of the hippocampal subregions and behavior.

Acknowledgments

This study was supported by project grants from Beijing Nova Program (xx2016120), National Natural Science Foundation of China (81101107, 31640035), Natural Science Foundation of Beijing (4162008) and program for Scientific Research Project of Beijing Educational Committee (SQKM201710005013).

References

[1] Maccotta L, Moseley ED, Benzinger TL, Hogan RE. Beyond the CA1 subfield: Local hippocampal shape changes in MRI-negative temporal lobe epilepsy. Epilepsia. 2015; 56:780–8.
[2] Wisse LEM, Gerritsen L, Zwanenburg JJM, Kuijf HJ, Luijten PR, Biessels GJ, et al. Subfields of the hippocampal formation at 7T MRI: In vivo volumetric assessment. NeuroImage. 2012;61:1043–9.
[3] Yuken F, Kazuo S, Masami M, Rokuro M, Kiminori I, Cairns NJ. Neurons and extracellular neurofibrillary tangles in the hippocampal subdivisions in early-onset familial Alzheimer's disease. A case study. Psychiatry Clin Neurosci. 2010; 51:227–31.
[4] Rössler M, Zarski R, Bohl J, Ohm TG. Stage-dependent and sector-specific neuronal loss in hippocampus during Alzheimer's disease. Acta Neuropathologica. 2002;103:363–9.
[5] de Flores R, Mutlu J, Bejanin A, Gonneaud J, Landeau B, Tomadesso C, et al. Intrinsic connectivity of hippocampal subfields in normal elderly and mild cognitive impairment patients: Hippocampal Subfields Connectivity. Human Brain Mapping. 2017;38:4922–32.
[6] Iglesias JE, Augustinack JC, Nguyen K, Player CM, Player A, Wright M, et al. A computational atlas of the hippocampal formation using ex vivo , ultra-high resolution MRI: Application to adaptive segmentation of in vivo MRI. NeuroImage. 2015;115:117–37.
[7] Aggleton JP. Multiple anatomical systems embedded within the primate medial temporal lobe: Implications for hippocampal function. Neurosci Biobehav Rev. 2012;36:1579–96.
[8] Shah P, Bassett DS, Wisse LEM, Detre JA, Stein JM, Yushkevich PA, et al. Mapping the structural and functional network architecture of the medial temporal lobe using 7T MRI. Human Brain Mapping. 2018;39:851–65.
[9] Wisse LEM, Biessels GJ, Geerlings MI. A Critical Appraisal of the Hippocampal Subfield Segmentation Package in FreeSurfer. Frontiers in Aging Neuroscience [Internet]. 2014 [cited 2018 Oct 9];6. Available from: http://journal.frontiersin.org/article/10.3389/fnagi.2014.00261/abstract
[10] Li W, Yang C, Shi F, Wu S, Wang Q, Nie Y, et al. Construction of Individual Morphological Brain Networks with Multiple Morphometric Features. Frontiers in Neuroanatomy [Internet]. 2017 [cited 2018 Jun 20];11. Available from: http://journal.frontiersin.org/article/10.3389/fnana.2017.00034/full
[11] Wu K, Taki Y, Sato K, Kinomura S, Goto R, Okada K, et al. Age-related changes in topological organization of structural brain networks in healthy individuals. Human Brain Mapping. 2012; 33:552–68.
[12] Hosseini SMH, Hoeft F, Kesler SR. GAT: A Graph-Theoretical Analysis Toolbox for Analyzing Between-Group Differences in Large-Scale Structural and Functional Brain Networks. Lambiotte R, editor. PLoS ONE. 2012; 7:e40709.
[13] Haneef Z, Lenartowicz A, Yeh HJ, Levin HS, Engel J, Stern JM. Functional connectivity of hippocampal networks in temporal lobe epilepsy. Epilepsia. 2014;55:137–45.
[14] Eklund A, Nichols TE, Knutsson H. Cluster failure: Why fMRI inferences for spatial extent have inflated false-positive rates. PNAS. 2016;201602413.
[15] Genovese CR, Lazar NA, Nichols T. Thresholding of Statistical Maps in Functional Neuroimaging Using the False Discovery Rate ☆. Neuroimage. 2002; 15:870–8.

[16] Bassett DS, Bullmore ET. Small-World Brain Networks Revisited. The Neuroscientist. 2017; 23:499–516.
[17] Sporns O, Tononi G. Structural Determinants of Functional Brain Dynamics. In: Jirsa VK, McIntosh A, editors. Handbook of Brain Connectivity [Internet]. Berlin, Heidelberg: Springer Berlin Heidelberg; 2007 [cited 2018 Oct 16]. p. 117–47. Available from: https://doi.org/10.1007/978-3-540-71512-2_4
[18] Achard S, Bullmore E. Efficiency and Cost of Economical Brain Functional Networks. PLoS Computational Biology. 2007; 3:e17.
[19] He Y, Chen Z, Evans A. Structural Insights into Aberrant Topological Patterns of Large-Scale Cortical Networks in Alzheimer's Disease. Journal of Neuroscience. 2008; 28:4756–66.
[20] Rubinov M, Sporns O. Complex network measures of brain connectivity: uses and interpretations. NeuroImage. 2010; 52:1059–69.
[21] Xia M, Wang J, He Y. BrainNet Viewer: A Network Visualization Tool for Human Brain Connectomics. PLOS ONE. 2013;8:e68910.
[22] Bernhardt BC, Chen Z, He Y, Evans AC, Bernasconi N. Graph-Theoretical Analysis Reveals Disrupted Small-World Organization of Cortical Thickness Correlation Networks in Temporal Lobe Epilepsy. Cerebral Cortex. 2011;21:2147–57.
[23] Watts DJ, Strogatz SH. Collective dynamics of 'small-world' networks. Nature. 1998;393:440–2.
[24] Betweenness Centrality Algorithms and Lower Bounds.pdf.
[25] Cheng H, Newman S, Goñi J, Kent JS, Howell J, Bolbecker A, et al. Nodal centrality of functional network in the differentiation of schizophrenia. Schizophrenia Research. 2015;168:345–52.
[26] Sporns O. The human connectome: A complex network. 2011.
[27] Wen W, Zhu W, He Y, Kochan NA, Reppermund S, Slavin MJ, et al. Discrete neuroanatomical networks are associated with specific cognitive abilities in old age. Journal of Neuroscience the Official Journal of the Society for Neuroscience. 2011;31:1204.
[28] Crossley NA, Mechelli A, Ginestet C, Rubinov M, Bullmore ET, McGuire P. Altered Hub Functioning and Compensatory Activations in the Connectome: A Meta-Analysis of Functional Neuroimaging Studies in Schizophrenia. Schizophrenia Bulletin. 2016;42:434–42.